# SIMULATION OF NATURAL CONVECTION OF NANOFLUIDS IN A SQUARE ENCLOSURE EMBEDDED WITH BOTTOM DISCRETE HEATER

by

***Siva Subrahmanyam MENDU[a*], Nagaraju DORA[b], and Megharaj Praneeth KARPURAPU[b]***

[a] Department of Mechanical Engineering, MVGR College of Engineering, Vizianagaram, India
[b] Department of Mechanical Engineering, Gitam University, Visakhapatnam, India

Original scientific paper
https://doi.org/10.2298/TSCI160413314M

*The present work aims at studying natural convection of nanofluids in a square enclosure embedded with a discrete heater at the bottom. The numerical simulations are performed using commercial software STAR CMM+ based on finite volume technique. Firstly, the results from the simulations are validated against the published results. Subsequently, numerical simulations have been carried out for predicting the flow and heat transfer characteristics of different water based nanofluids ($Al_2O_3$, Cu, $TiO_2$) at wide range of Rayleigh numbers, volume fractions, position of the heater and heater length. Results are presented in the form of streamline plots, isotherm contours and plots of average Nusselt numbers. It has been found that the average Nusselt number increases with increasing Rayleigh number, volume fraction, and heater length. Further, the effect of heater position on the flow and temperature fields for different nanofluids are discussed. However, Nusselt number was observed to be sensitive to the position of the heater.*

Key words: *natural convection, CFD, nanofluid, square enclosure with bottom heater,*

## Introduction

Natural convection in enclosures is an important aspect in many heat transfer applications. Designing of an efficient heat transfer system is of prime concern in many of the contemporary engineering applications like the electronic cooling systems [1]. Conventionally, fluids such as water, oils, ethylene glycol, *etc*., used in such applications achieve low heat transfer rates due to their lower thermal conductivity. Several new techniques based on extended surfaces, turbulators, *etc*., have been developed for the enhancement of heat transfer. However, these developments were not adequate in meeting the requirements of higher heat transfer rates. In order to achieve the said requirement, the authors felt it is desirable to improve the thermal properties of fluids. This could be achieved by dispersing nanometallic particles in the base fluids known the nanofluids. Several studies have been done on simulation of natural convection using nanofluids in different wall bounded enclosure configurations.

Khanafer *et al.* [2] studied natural convection of nanofluids in a 2-D enclosure using finite volume method. They analyzed the flow and heat transfer behavior of nanofluids inside a

* Corresponding author, e-mail: m.sivasubrahmanyam@gmail.com

rectangular enclosure with differentially heated side walls. Jou and Tzeng [3] used finite difference method for studying the flow and heat transfer inside a rectangular enclosure filled with nanofluids. They studied the effect of volume fraction, Rayleigh number and aspect ratio on flow pattern and heat transfer rate.

In the recent years, several investigations have been done on simulation of convective heat transfer of nanofluids inside a differentially heated side wall [4, 5] and bottom wall enclosure [6-11]. Though the previous literature mainly focuses on natural convection in an enclosure with differentially heated walls either vertical or bottom heated walls, few studies have been done on the study of natural convection in enclosure with partially heated walls.

Natural convection in a partially heated enclosure has received considerable interest due to their wide applications in buildings and electronic cooling. Several studies have been done on simulation of natural convection filled with conventional fluids in rectangular enclosures embedded with partial heaters [12-15]. Natural convection of nanofluids in a partially heated and cooled square enclosure was studied by Das and Ohal [16]. In their study, the finite volume approach was used to simulate the flow and heat transfer for different volume fractions and values of Rayleigh number. Later, Oztop and Abu-Nada [17] employed the same method to simulate three distinct nanofluids (Cu, $Al_2O_3$, $TiO_2$) inside a rectangular enclosure with partially heated side wall. They studied the effect of heater height, location of heater, volume fraction, Rayleigh number, and aspect ratio on the fluid-flow and heat transfer.

The literature is mainly focused on natural convection of nanofluids in enclosure with partially heated side walls. To the best of the author's knowledge, no studies have been reported on study of natural convection of nanofluids inside square enclosure with partially heated bottom wall. In the present study natural convection of nanofluids inside a partially heated bottom wall filled with nanofluids is simulated. A finite volume based commercial software STAR CCM+ is used for analyzing flow and heat transfer inside a square enclosure at different values of Rayleigh number, nanofluids, volume fractions, length of the heater, and position of the heater.

## Physical model

The physical model of the partially heated square enclosure filled with nanofluids embedded with bottom heater is shown in fig.1. The temperature of the partial heater at the bottom wall and upper cold wall is maintained at a constant temperature of $T_h$ and $T_c$, respectively, while the other walls are well insulated. The enclosure is filled with Cu, $Al_2O_3$, $TiO_2$ water based nanofluids. The following assumptions have been made in the present analysis.

- The flow is laminar, 2-D, incompressible and in steady-state.
- The fluid is considered to be Newtonian.
- The thermal and physical properties of nanofluids are independent of temperature except the variation in density.
- The shape and size of the nanoparticle are assumed to be uniform.
- The shape of nanoparticles is spherical.
- Thermal equilibrium is assumed to be achieved for both water and nanoparticles.

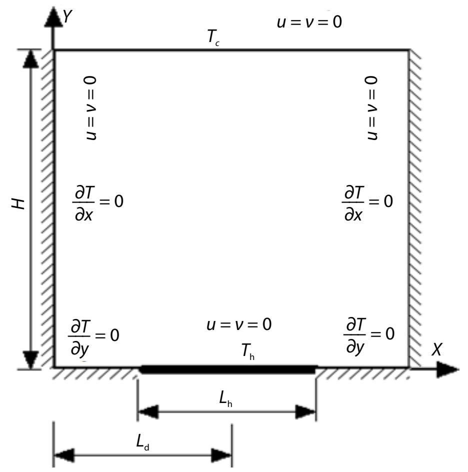


**Figure 1. The physical model of partially heated 2-D square enclosure filled with nanofluids**

– Negligible radiation heat transfer when compared to other modes of heat transfer.
– Negligible viscous heat dissipation.

### *Governing equations and boundary conditions*

Considering the aforementioned assumptions, the reduced governing equations (mass, momentum, and energy) for 2-D flows are given:

$$\frac{\partial u}{\partial x}+\frac{\partial v}{\partial y}=0 \tag{1}$$

$$u\frac{\partial u}{\partial x}+v\frac{\partial u}{\partial y}=-\frac{1}{\rho_{\mathrm{nf}}}\frac{\partial p}{\partial x}+\frac{\mu_{\mathrm{nf}}}{\rho_{\mathrm{nf}}}\left(\frac{\partial^2 u}{\partial x^2}+\frac{\partial^2 u}{\partial y^2}\right) \tag{2}$$

$$u\frac{\partial v}{\partial x}+v\frac{\partial v}{\partial y}=-\frac{1}{\rho_{\mathrm{nf}}}\frac{\partial p}{\partial y}+\frac{\mu_{\mathrm{nf}}}{\rho_{\mathrm{nf}}}\left(\frac{\partial^2 v}{\partial x^2}+\frac{\partial^2 v}{\partial y^2}\right)+\mathrm{g}_y\beta\left(T-T_{\mathrm{ref}}\right) \tag{3}$$

$$u\frac{\partial T}{\partial x}+v\frac{\partial T}{\partial y}=\alpha\left(\frac{\partial^2 T}{\partial x^2}+\frac{\partial^2 T}{\partial y^2}\right) \tag{4}$$

In the view of importance of the boundary conditions, isothermal boundary conditions were imposed on heater and cold wall. The other walls are assumed to be adiabatic. The boundary conditions are shown in fig. 1. The bottom wall is embedded with heater partly and it is maintained at constant temperature for various heater lengths. The enclosure is filled with nanofluids and it is assumed that both base fluid (water) and nanoparticles are in thermal equilibrium.

### *Thermo physical properties of nanofluids*

Thermo physical properties of nanofluid have been calculated using the following correlations:

– The density of nanofluid is given [7]:

$$\rho_{\mathrm{nf}}=(1-\phi)\rho_{\mathrm{bf}}+\phi\rho_{\mathrm{p}} \tag{5}$$

– The heat capacitance of the nanofluid is expressed [2]:

$$(\rho c_p)_{\mathrm{nf}}=(1-\phi)(\rho c_p)_{\mathrm{bf}}+\phi(\rho c_p)_{\mathrm{p}} \tag{6}$$

– The thermal expansion coefficient, $\beta$, of a nanofluid can be determined [7]:

$$(\rho\beta)_{\mathrm{nf}}=(1-\phi)(\rho\beta)_{\mathrm{bf}}+\phi(\rho\beta)_{\mathrm{p}} \tag{7}$$

– The effective thermal conductivity, $k_{\mathrm{nf}}$, of the nanofluid is approximated by the Maxwell-Garnett's model [1, 15, 17-20]:

$$k_{\mathrm{nf}}=k_{\mathrm{bf}}\left[\frac{k_{\mathrm{p}}+2k_{\mathrm{bf}}-2\phi(k_{\mathrm{bf}}-k_{\mathrm{p}})}{k_{\mathrm{p}}+2k_{\mathrm{bf}}+\phi(k_{\mathrm{bf}}-k_{\mathrm{p}})}\right] \tag{8}$$

where $k$ is the thermal conductivity.

– The viscosity, $\mu_{\mathrm{nf}}$, of the nanofluid can be calculated [17]:

$$\mu_{\mathrm{nf}}=\frac{\mu_{\mathrm{bf}}}{(1-\phi)^{2.5}} \tag{9}$$

**Table 1. Thermo physical properties of base fluid and nano particles [17]**

| Parameter | Base fluid (water) | Cu | $Al_2O_3$ | $TiO_2$ |
|---|---|---|---|---|
| $C_p$ [$Jkg^{-1}K^{-1}$] | 4179 | 385 | 765 | 686.2 |
| $\rho$ [$kgm^{-3}$] | 997.1 | 8933 | 3970 | 4250 |
| $k$ [$wm^{-1}K^{-1}$] | 0.613 | 400 | 40 | 8.953 |
| $\beta \cdot 10^{-5}$ [$1K^{-1}$] | 21 | 1.67 | 0.85 | 0.901 |
| $\alpha \cdot 10^{-7}$ [$m^2s^{-1}$] | 1.47 | 1163.1 | 131.7 | 30.70 |

– The thermal diffusivity can be expressed:

$$\alpha_{\mathrm{nf}} = \frac{k_{\mathrm{nf}}}{(\rho c_p)_{\mathrm{nf}}} \tag{10}$$

The thermo physical properties of fluids used in the present study are shown in tab.1.

*Governing parameters*

The following governing parameters are used in the present analysis:

– Prandtl number $$\mathrm{Pr_{nf}} = \frac{\mu_{\mathrm{nf}} c_{p(\mathrm{nf})}}{k_{\mathrm{nf}}} \tag{11}$$

– Rayleigh number $$\mathrm{Ra_{nf}} = \frac{\rho_{\mathrm{nf}} \mathrm{g} \beta_{\mathrm{nf}} \Delta T H^3}{\mu_{\mathrm{nf}} \alpha_{\mathrm{nf}}} \tag{12}$$

The average Nusselt number on heater can be determined:

$$\overline{\mathrm{Nu}} = \frac{\int_{L_d - \frac{L_h}{2}}^{L_d + \frac{L_h}{2}} \mathrm{Nu}_y \mathrm{d}x}{\int_{L_d - \frac{L_h}{2}}^{L_d + \frac{L_h}{2}} \mathrm{d}x} \tag{13}$$

where $\mathrm{Nu}_y$ is the local Nusselt number and it can be expressed:

$$\mathrm{Nu}_y = -\frac{L}{T_\mathrm{h} - T_\mathrm{c}} \frac{\partial T}{\partial y}$$

## Computational procedure

The governing eqs. (1)-(4) were solved using the finite volume based commercial software STAR CCM+. At first the geometry is created and materials are assigned to the components. The boundary conditions are imposed on the walls. The structured mesh is generated and prismatic layer mesh is used. Prism layers are generated near the wall to capture the thin boundary-layers at higher values of Rayleigh numbers. In the present analysis a two 2-D, steady, laminar, coupled flow, coupled energy, gravity, and Boussinesq approximation models were chosen to simulate natural convection inside an enclosure with embedded partial heater at the bottom wall. Simulations have been run up to 5000 iterations in order to get the converged solution within the tolerance of 1e-8.

*Grid independence test and validation*

Natural convection in a differentially heated side walls filled with water was considered for grid independence test, prior to performing the actual simulations with nanofluids.

Three different grid sizes such as 80 × 80, 160 × 160, and 320 × 320 were considered. The grid refinement tests were conducted for different values of Ra ($10^3$, $10^4$, and $10^5$). In the view of grid independence, convergence and computational accuracy, a very popular Richardson extrapolation technique has been adopted [18, 21-23]. The relation is given by:

$$I_{\rm ext} = I_{\rm M3} + \frac{I_{\rm M3} - I_{\rm M2}}{r^p - 1} \tag{14}$$

where the ratio of coarse to fine grid spacing is represented as $r = 2$ and extrapolation accuracy as $p = 2$. The variation of average Nusselt number with grid refinement for Ra = $10^4$ and $10^5$ has been tabulated in tab. 2 along with % error. It is perceived from tab. 2 that the results are in good agreement between grid sizes 160 × 160 and 320 × 320. Further, the percentage of error decreases as grid size increases. Hence, the grid size 160 × 160 has been selected in the present work in view of good accuracy and computational time.

**Table 2. The variation of average Nusselt number with grid refinement for different values of Rayleigh number**

| | Ra = $10^4$ | | | Ra = $10^5$ | | |
|---|---|---|---|---|---|---|
| | M1 (80 × 80) | M2 (160 × 160) | M3 (320 × 320) | M1 (80 × 80) | M2 (160 × 160) | M3 (320 × 320) |
| $I$ | 2.2691 | 2.2710 | 2.2721 | 4.7130 | 4.7210 | 4.7229 |
| $I_{\rm ext}$ | 2.2725 | | | 4.7235 | | |
| % Error | 0.149 | 0.066 | 0.017 | 0.22 | 0.053 | 0.013 |

Further, the differentially heated square enclosure [24] filled with water based $Al_2O_3$ nanofluid was considered to validate the simulated results for different values of Rayleigh number and volume fraction. The obtained Nusselt numbers on heated wall were validated against the published results of Ternik *et al.*, [24]. The results are in good agreement with that of published results and the comparison has been shown in tab. 3.

**Table 3. Average Nusselt number values for natural convection flow in a differentially heated square enclosure filled with $Al_2O_3$-water nanofluid for various volume concentrations**

| $\phi$ | $10^3$ | | % Error | $10^4$ | | % Error | $10^5$ | | % Error |
|---|---|---|---|---|---|---|---|---|---|
| | [24] | Present | | [24] | Present | | [24] | Present | |
| 0.01 | 1.1490 | 1.1493 | 0.02 | 2.3431 | 2.3412 | 0.08 | 4.8951 | 4.8864 | 0.17 |
| 0.02 | 1.1825 | 1.1836 | 0.09 | 2.4098 | 2.4065 | 0.13 | 4.9943 | 4.9920 | 0.04 |
| 0.03 | 1.2181 | 1.2190 | 0.07 | 2.4798 | 2.4784 | 0.05 | 5.1408 | 5.1481 | 0.14 |
| 0.04 | 1.2523 | 1.2567 | 0.35 | 2.5498 | 2.5508 | 0.39 | 5.2873 | 5.2828 | 0.08 |
| 0.05 | 1.2879 | 1.2811 | 0.52 | 2.6197 | 2.6147 | 0.19 | 5.4281 | 5.4244 | 0.06 |

## Results and discussion

In the present study, simulations have been carried out for different nanofluids in order to study the influence of various parameters such as Rayleigh number, volume fraction, $\phi$, heater position, $L_d$, and heater length, $L_h$, on flow and heat transfer characteristics inside an enclosure.

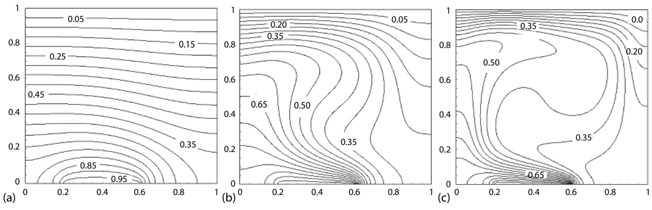


**Figure 2. Comparison of isotherms for $TiO_2$-water nanofluid at $L_d$ = 0.4, $\phi$ = 5%, $L_h$ = 0.4 H for different values of Rayleigh number; (a) Ra = $10^3$, (b) Ra = $10^4$ , and (c) Ra = $10^5$**

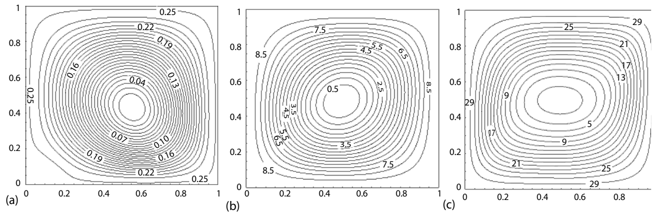


**Figure 3. Stream line plots for $TiO_2$-water nanofluid at $L_d$ = 0.4, $\phi$ = 5%, $L_h$ = 0.4 H for different values of Rayleigh numbers; Ra = (a) $10^3$, (b) $10^4$, and (c) $10^5$**

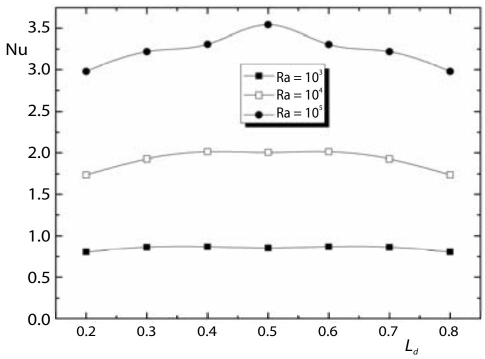


**Figure 4. Average Nusselt number *vs.* $L_d$ for different Ra at $\phi$ = 5% and $TiO_2$-water nanofluid**

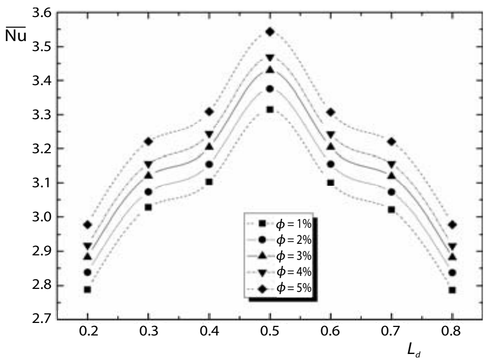


**Figure 5. Variation of average Nusselt number over different heater positions $L_d$ for different $\phi$ at Ra = $10^5$, $TiO_2$-water nanofluid, $L_h$= 0.4 H**

### *Effect of Rayleigh number*

The variation of temperature field has been analyzed for different values of Rayleigh number. For the sake of brevity the results have been presented only for $TiO_2$-water based nanofluid, $L_d$ = 0.4, $\phi$ = 5%, and $L_h$ = 0.4 H, fig. 2. It is seen from fig. 2 that a thin boundary-layer is formed on the surface of the bottom heater and the top cold wall as Rayleigh number increases from $10^3$-$10^5$. This is due to the fact that the tightly packed isotherms create large temperature gradients and augment the convective heat transfer. This indicates that the buoyancy is increased. The values of stream function have shown in fig. 3 support the statement.

The fig. 4 shows the effect of Rayleigh number on the variation of average Nusselt number. It is observed that the Nusselt number increases as heater moves towards the center of heater from the left side wall at different values of Rayleigh number ($10^3$-$10^5$). This indicates that the heat transfer is enhanced with the increase of Rayleigh number as expected. It is also depicted from fig. 4 that the maximum value of the average Nusselt number attained at $L_d$ = 0.5 as Rayleigh number increases to $10^5$.

### *Effect of volume fraction*

In the present section, five volume fractions ($\phi$ = 1% to 5%) for three different water based nanofluids such as $Al_2O_3$, Cu, and $TiO_2$ were considered for investigating their effects on average Nusselt number. The simulations were conducted for different combinations of parameters. For the compactness, the results of $TiO_2$-water nanofluid were presented for different volume fractions at Ra = $10^5$ and $L_h$ = 0.4 H.

The fig. 5 shows that the average Nusselt number increases with increasing volume fraction from 1-5%. This is due to the fact that the motion of ultra-fine nanoparticles (Cu, $Al_2O_3$, and $TiO_2$) at high volume fractions causes high energy transport through fluid-flow. It is evident that as volume fraction increases from 1% to 5%, the values of Prandtl number changes from 5.86-5.17. This indicates that the dominance behavior of thermal diffusivity over momentum diffusivity causes higher values of Nusselt number.

### *Effect of nanofluid*

The heat transfer enhancement is strongly depends on the usage of different types of nanofluids and such fluids are used as working fluids in the real time applications. In the present section, simulations have been done for three different types of water based nanofluids ($Al_2O_3$, $TiO_2$, and Cu) by keeping other parameters remains constant. The effect of volume fraction on different heater positions is observed and the Nusselt number is attained maximum at $L_d = 0.5$ for all volume fractions. Results have been presented at Ra = $10^5$, $L_h = 0.4$ H and $L_d = 0.4$. It can be seen that the average Nusselt number is observed as maximum for Cu nanofluid for the given volume fraction range ($1\% \leq \phi \leq 5\%$) and the minimum Nusselt number is attained for $TiO_2$ as shown in fig. 6.

As it is well known that the thermal conductivity of $Al_2O_3$ is approximately one tenth of Cu, due to low thermal diffusivity of $Al_2O_3$, the temperature gradients may be high but poor thermal conductivity affects the average Nusselt number. However, the higher thermal conductivity at wide range of volume fractions for Cu based nanofluids augments the average Nusselt number. It is also observed that the mean Nusselt number diminishes for $TiO_2$ nanofluid due to its less thermal conductivity than Cu and $Al_2O_3$.

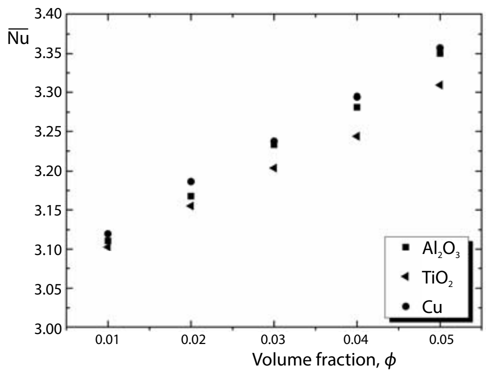


**Figure 6. Variation of average Nusselt number or Cu, $Al_2O_3$, and $TiO_2$-water based nanofluids at Ra = $10^5$, $L_d = 0.4$ and $L_h = 0.4$ H**

### *Effect of heater position*

The effect of heater position also has the importance to study the variation of heat transfer inside enclosure and the intensity of the convection in the enclosure is much more influenced by the position of the heater at the bottom wall. In this regard, simulations were conducted at different values of Rayleigh number as the heater moves from the left wall towards the right wall. Seven different positions have been considered to analyze the convective flow and heat transfer characteristics.

From fig. 7, it is seen that the growth of thermal boundary-layer on surface of the heater increases as the heater moves towards the center from the left wall and conversely, the growth has been reduced when the heater moves from the center towards the right wall.

This is due to the fact that the adiabatic wall blocks the natural convective flow as the heater moves towards the walls. The same phenomena can be observed in fig. 8. The variation of average Nusselt number on heater has been traced for nanofluids at different positions, $L_d$. It is seen that the Nusselt number increases as the heater moves towards the centre and shows the symmetry behavior about y-axis at position $L_d = 0.5$ for all Rayleigh number numbers, also the same is reconfirmed by figs. 7-9.

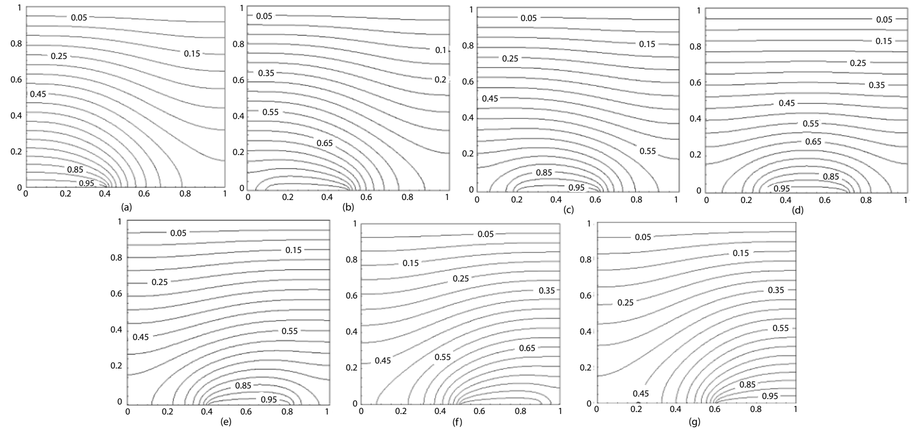

**Figure 7. Isotherms for $TiO_2$-water nanofluid at Ra = $10^3$, $\phi$ = 5%, $L_h$ = 0.4 H with different heater positions $L_d$ = 0.2 (a), 0.3 (b), 0.4 (c), 0.5 (d), 0.6 (e), 0.7 (f), and 0.8 (g)**

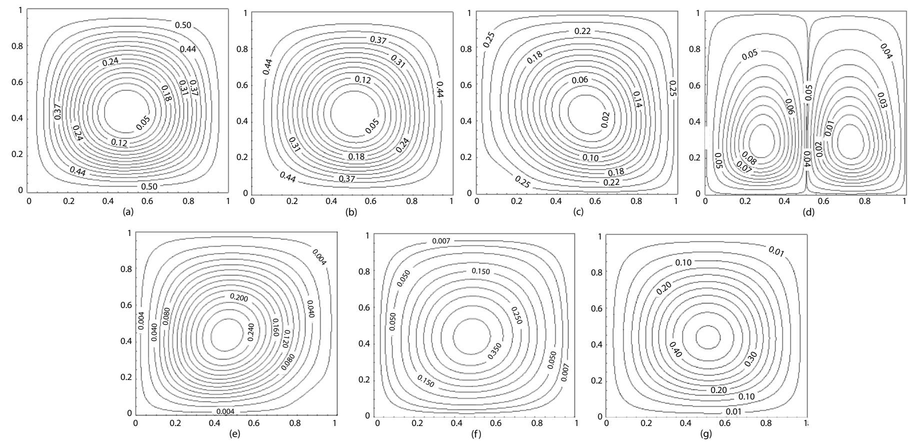

**Figure 8. Stream line plots for $TiO_2$-water nanofluid at Ra = $10^3$, $\phi$ = 5%, $L_h$ = 0.4 H with different heater positions $L_d$ = 0.2 (a), 0.3 (b), 0.4 (c), 0.5 (d), 0.6 (e), 0.7 (f), and 0.8 (g)**

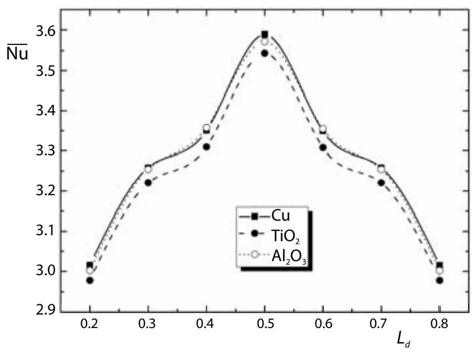


**Figure 9. The average Nusselt number *vs.* $L_d$ for different nanofluids at $\phi$ = 5%, Ra = $10^5$, and $L_h$= 0.4 H**

### *Effect of heater length*

In the previous sections, investigations have been done for fixed heater length ($L_h$ = 0.4 H). It is well known fact that the flow and temperature distribution, and eventually heat transfer at the enclosure walls will depend on the length of the heater. In view of the mentioned information, it is necessary to study the variation of temperature distribution, flow, and average Nusselt number for different heater lengths. In the present work, two heater lengths $L_h$= 0.4 H and 0.2 H has been considered and numerical investigations are done for all nanofluids by keeping all other parameters remains fixed.

Keeping in view of the compactness, the results of $L_d = 0.5$, $\phi = 5\%$, Ra = $10^5$ and $TiO_2$-water nanofluid have been presented. It is revealed from fig. 10 that the temperature distribution is enhanced as the length of the heater increases. The streamline plots shown in fig. 11 support the previous observations. The similar trend can be observed in the case of streamline distribution as shown in fig. 11. It can be seen the streamline plots have not shown any difference in their flow patterns. However, circulation is much weaker for $L_h$= 0.2 H. The stream function values in fig. 11 reconfirm that. Further, the variation of average Nusselt number has been plotted for the two heater lengths. Figure 12 depicts the variation of average Nusselt number. It is expected that the average Nusselt number increases with the increase of heater length due to the increase in heat transfer surface area.

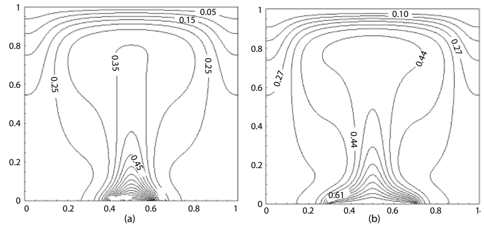

**Figure 10. Isotherms for $TiO_2$-water based nanofluid at Ra = $10^5$, $\phi = 5\%$, $L_d = 0.5$ with different $L_h = 0.2$ H (a), 0.4 H (b)**

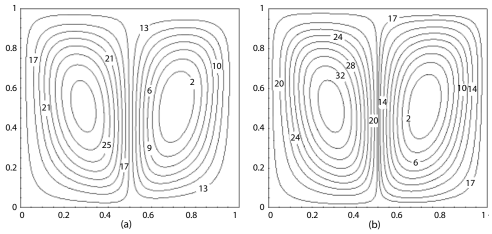

**Figure 11. Stream line path for $TiO_2$-water based nanofluid at Ra = $10^5$, $\phi = 5\%$, $L_d = 0.5$ with different $L_h = 0.2$ H (a), 0.4 H (b)**

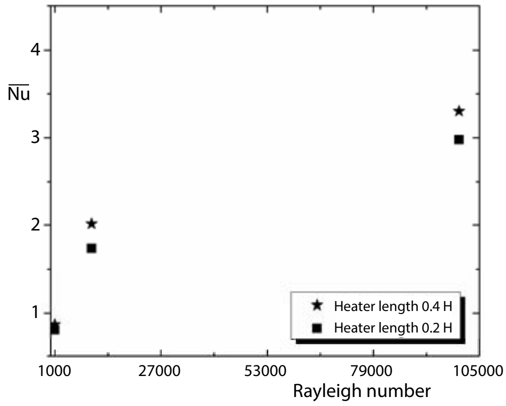


**Figure 12. Variation of average Nusselt number with Rayleigh number for different heater lengths at $TiO_2$-water based nanofluid, $\phi = 5\%$, and $L_d = 0.5$**

## Conclusions

The CFD simulations of natural convection of water based nanofluids in a square enclosure embedded with a partially heated bottom wall were carried out using commercial software STAR CCM+. The effect of Rayleigh number, volume fraction, nanoparticle, and heater length along with its position is studied to predict the flow and heat transfer characteristics. The following conclusions have been drawn from the obtained results.

- Natural convection heat transfer in enclosure is intensified as the value of Rayleigh number increases.
- As volume fraction increases from 1-5%, the average Nusselt number is increased.
- The Cu-water based nanofluid has shown higher Nusselt number compared to $TiO_2$ and $Al_2O_3$ water based nanofluid.
- The position of the heater is an important parameter for enhancing the heat transfer. The value of Nusselt number increases as the heater position moves towards the center of the enclosure. The maximum Nusselt number is seen at $L_d = 0.5$ for different nanofluids.
- Isotherms and streamline plots have shown the higher intensity of heat transfer and flow field at $L_d = 0.5$.
- The average Nusselt number has been enhanced at larger heater lengths for all combinations of simulated parameters.

## Nomenclature

$c_p$ – specific heat, [$Jkg^{-1}K^{-1}$]
g – acceleration due to gravity, [$ms^{-2}$]
$H$ – height of enclosure, [m]
$I$ – converged $\overline{Nu}$ [–]
$I_{ext}$ – Richardson extrapolation, [–]
$k$ – thermal conductivity, [$Wm^{-1}K^{-1}$]
$L$ – length of enclosure, [m]
$L_d$ – heater position, [–]
$L_h$ – length of heater, [m]
$u$, $v$ – x, y component of velocity, [$ms^{-1}$]
Nu – local Nusselt number [–]
$\overline{Nu}$ – average Nusselt number, [–]
Pr – Prandtl number
$T$ – temperature, [K]

*Greek symbols*

$\mu$ – dynamic Viscosity, [Pa s]
$\phi$ – volume concentration, [–]
$\alpha$ – thermal diffusivity, [$m^2s^{-1}$]
$\beta$ – thermal expansion coefficient, [$K^{-1}$]
$\rho$ – density, [kg $m^{-3}$]

*Subscripts*

bf – base fluid
nf – nanofluid
p – solid particle
c, h – cold and hot
M – mesh size

## References

[1] Abu-Nada, E., Application of Nanofluids for Heat Transfer Enhancement of Separated Flow Encountered in a Backward Facing Step, *Int. J. Heat Fluid Flow*, *29* (2008), 1, pp. 242-249
[2] Khanafer, K., *et al*., Buoyancy-Driven Heat Transfer Enhancement in a Two-Dimensional Enclosure Utilizing Nanofluids, *Int. J. Heat Mass Transf*., *46* (2003), 19, pp. 3639-3653
[3] Jou, R.-Y., Tzeng, S.-C., Numerical Research of Nature Convective Heat Transfer Enhancement Filled with Nanofluids in Rectangular Enclosures, *Int. Commun. Heat Mass Transf*., *33* (2006), 6, pp. 727-736
[4] Abu-Nada, E., *et al*., Effect of Nanofluid Variable Properties on Natural Convection in Enclosures, *Int. J. Thermal Science*, *49* (2010), 3, pp. 479-491
[5] Tiwari, R. K., Das, M. K., Heat Transfer Augmentation in a Two-Sided Lid-Driven Differentially Heated Square Cavity Utilizing Nanofluids, *Int. J. Heat Mass Transf*., *50* (2007), 9-10, pp. 2002-2018
[6] Jang, S. P., *et al*., Particle Concentration and Tube Size Dependence of Viscosities of $Al_2O_3$-Water Nanofluids Flowing through Micro- and Mini-tubes, *Appl. Phys. Lett*., *91* (2007), 24, 243112
[7] Lai, F.-H., Yang, Y.-T., Lattice Boltzmann Simulation of Natural Convection Heat Transfer of $Al_2O_3$-Water Nanofluids in a Square Enclosure, *Int. J. Therm. Sci*., *50* (2011), 10, pp. 1930-1941
[8] Parvin, S., *et al*., Double-Diffusive Natural Convection in a Partially Heated Enclosure Using a Nanofluid, *Heat Transfer-Asian Res*., *41* (2012), 6, pp. 484-497
[9] Rashmi, W., *et al*., CFD Studies on Natural Convection Heat Transfer of $Al_2O_3$-Water Nanofluids, *Heat Mass Transf*., *47* (2011), 10, pp. 1301-1310
[10] Santra, A. K., *et al*., Study of Heat Transfer Augmentation in a Differentially Heated Square Cavity Using Copper-Water Nanofluid, *Int. J. Therm. Sci*., *47* (2008), 9, pp. 1113-1122
[11] Wang, X. Q., *et al*., Free Convection Heat Transfer in Horizontal and Vertical Rectangular Cavities Filled with Nanofluids, Begell House Inc., *Proceedings*, International Heat Transfer Conference IHTC-13, Sydney, Australia, 2006
[12] Chao, P. K.-B., Laminar Natural Convection in an Inclined Rectangular Box with the Lower Surface Half-Heated and Half-Insulated, *J. Heat Transf*., *105* (1983), 3, pp. 425-432
[13] Orhan, A., Yang, W. J., Natural Convection in Enclosures with Localized Heating from Below and Symmetrical Cooling from Sides, *Int. J. Numer. Methods Heat Fluid Flow*, *10* (2000), 5, pp. 518-529
[14] Ishihara, I., *et al*., Natural Convection in a Vertical Rectangular Enclosure with Symmetrically Localized Heating and Cooling Zones, *Int. J. Heat Fluid Flow*, *23* (2002), 3, pp. 366-372
[15] Ahmet Koca, H. F. O., The Effects of Prandtl Number on Natural Convection in Triangular Enclosures with Localized Heating from below, *Int. Commun. Heat Mass Transf*., *34* (2007), 4, pp. 511-519
[16] Das, M. K., Ohal, P. S., Natural Convection Heat Transfer Augmentation in a Partially Heated and Partially Cooled Square Cavity Utilizing Nanofluids, *Int. J. Numer. Methods Heat Fluid Flow*, *19* (2009), 3/4, pp. 411-431
[17] Oztop, H. F., Abu-Nada, E., Numerical Study of Natural Convection in Partially Heated Rectangular Enclosures Filled with Nanofluids, *Int. J. Heat Fluid Flow*, *29* (2008), 5, pp. 1326-1336
[18] Ternik, P., Rudolf, R., Conduction and Convection Heat Transfer Characteristics of Water-Based Au Nanofluids in a Square Cavity with Differentially Heated Side Walls Subjected to Constant Temperatures, *Thermal Science, 18* (2014), Suppl. 1, pp. S189-S200

[19] Malga, S. E. B., *et al*., Heat Transfer Enhancement by Using Nanofluids in Forced Convection Flows, *Int. J. Heat Fluid Flow*, *26* (2005), 4, pp. 530-546
[20] Palm, S. J., *et al*., Heat Transfer Enhancement with the Use of Nanofluids in Radial Flow Cooling Systems Considering Temperature-Dependent Properties, *Appl. Therm. Eng*., *26* (2006), 17-18, pp. 2209-2218
[21] Ternik, P., Conduction and Convection Heat Transfer Characteristics of Water-Au Nanofluid in a Cubic Enclosure with Differentially Heated Side Walls, *Int. J. Heat Mass Transf.*, *80* (2015), Jan., pp. 368-375
[22] Ternik, P., Rudolf, R., Numerical Analysis of Continuous Casting of NiTi Shape Memory Alloy, *Int. J. Simul. Model.*, *15* (2016), 3, pp. 522-531
[23] Ternik, P., *et al.*, Numerical Stady of Heat-Transfer Enhancement of Homogeneous of Water-Au Nanofluid under Natural Convection, *Mater. Tehnol*., *46* (2012), 3, pp. 257-261
[24] Ternik, P., Rudolf, R., Heat Transfer Enhancement for Natural Convection Flow of Water Based Nanofluids in a Square Enclosure, *Int. J. Simul. Model.*, *11* (2012) 1, pp. 29-39

Paper submitted: April 13, 2016
Paper revised: November 28, 2016
Paper accepted: December 23, 2016